Global and Planetary Change 208 (2022) 103701

Contents lists available at ScienceDirect

Global and Planetary Change

journal homepage: www.elsevier.com/locate/gloplacha

Research article

Ancient climate changes and Andes uplift, rather than Last Glacial Maximum, affected distribution and genetic diversity patterns of the southernmost mycoheterotrophic plant *Arachnitis uniflora* Phil. (Corsiaceae)

Mauricio Renny [a,*], M. Cristina Acosta [a,b,1], Alicia N. Sérsic [a,1]

[a] *Instituto Multidisciplinario de Biología Vegetal, IMBIV, UNC-CONICET, Edificio de Investigaciones Biológicas y Tecnológicas, Vélez Sársfield 1611, 5000 Córdoba, Argentina*

[b] *Facultad de Ciencias Exactas, Físicas y Naturales, Universidad Nacional de Córdoba, Argentina*

ARTICLE INFO

Editor: Fabienne Marret-Davies

Keywords:
Arachnitis uniflora
Mycoheterotrophy
Andean–Patagonian forest
Andean uplift
Genetic diversity
Great Patagonian Glaciation

ABSTRACT

Arachnitis uniflora (Corsiaceae) is a mycoheterotrophic plant native to South America that grows in tropical semi-humid forests of Peru and Bolivia, in the temperate Andean-Patagonian forests of Argentina and Chile, and in the moorlands of Malvinas/Falkland Islands. This widely distributed and disjunct species offers the opportunity to explore the dynamics of evolutionary processes using phylogeographic approaches, spatio-temporal and paleo-distribution reconstructions; these tools allow us to test how ancient geological events and climate changes occurred in the Miocene-Pliocene and how the more recent Pleistocene events affected diversification, demography, and genetic diversity patterns over space and time. We sampled 28 sites, covering the whole geographic range of *Arachnitis uniflora*. We amplified and sequenced the internal transcribed spacer (ITS), 18S rRNA, and 26S rRNA nuclear regions in 141 individuals, and the plastid 16S rRNA gene in a subset of 90 individuals. In order to reconstruct the evolutionary history of the species, we performed phylogeographic, dating analyses, spatio-temporal diffusion models, and species paleo-distribution projections. *Arachnitis uniflora* has an ancient origin and diversified during the Late Miocene, splitting into two genetic groups named the Northern and Patagonian groups. Haplotype diversification of both groups dated about late Miocene and early Pliocene. We detected demographic expansion at the early Pleistocene, and most diversifications and colonizations occurred before the LGM. Paleo-distribution modelling predicted few changes of the species distribution from 800 Mya to the present, showing only a range expansion at the east during the LGM. Four areas of high genetic diversity were identified suggesting refugial areas where the species persisted. Orogeny and climate changes promoted by the Andes uplift during the Late Miocene produced the main ancient genetic divergence due to the formation of the Arid Diagonal. Most diversification, colonizations, and demographic processes occurred from early Pliocene to the beginning of the Pleistocene before the Great Patagonian Glaciation, revealing a low influence of the LGM glaciations on the species evolutionary history.

1. Introduction

Knowledge about the processes involved in the current geographical distribution of a species lineages needs a rigorous approach into their evolutionary history and especially into the role of landscape changes in genetic diversity patterns at intraspecific level (Hewitt, 1996; Hutchinson and Templeton, 1999; Davis and Shaw, 2001). In South America, geological events and past climatic changes affected biogeographic patterns, demography and lineage differentiation within species (Ortiz-Jaureguizar and Cladera, 2006; Hoorn et al., 2010). According to Villagrán and Hinojosa (1997), a disruption in the floristic interchange between current subtropical regions and the Andean-Patagonian areas began at the end of the Eocene, when the opening of the Drake passage promoted glaciations in the Antarctica and a global cooling (Ortiz-Jaureguizar and Cladera, 2006; Zachos et al., 2008). In addition, early Andean uplift events occurred from the Eocene and the occurrence of marine transgressions recorded in the Oligocene of southern South-America could have acted as efficient genetic barriers (Ortiz-

* Corresponding author.
E-mail address: bio.mrenny@gmail.com (M. Renny).
[1] These authors contributed equally to this work

https://doi.org/10.1016/j.gloplacha.2021.103701
Received 1 September 2020; Received in revised form 8 October 2021; Accepted 5 November 2021
Available online 13 November 2021

Jaureguizar and Cladera, 2006; Premoli et al., 2012; Bechis et al., 2014; Quiroga et al., 2015).

The Andean uplift episode called Inca phase (37 Mya; Eocene; see Yrigoyen, 1979) triggered the development of the Bolivian oroclinal in the central Andes (Ortiz-Jaureguizar and Cladera, 2006; O'Driscoll et al., 2012). During late Oligocene–Early Miocene (ca. 26–20 Ma), the present morpho-structural configuration of the Andes of Central Chile began to develop. At the end of the Quechua phase (11-7 Mya; Miocene), the uplift of the southern Andes produced a rain shadow that prevented the entry of the humid westerlies from the Pacific Ocean, causing the desertification of the eastern plains (Ortiz-Jaureguizar and Cladera, 2006). Thus, the formation of the Arid Diagonal during the end of the Miocene would have acted as a drastic barrier to vegetation interchanges (Villagrán and Hinojosa, 1997). The Arid Diagonal extends along the Patagonian steppes, the Monte ecoregion, and on the Pacific coast from the 30°S up to 5°S, in Ecuador (Hueck, 1978; Villagrán and Hinojosa, 1997; Ortiz-Jaureguizar and Cladera, 2006; Ramos and Ghiglione, 2008). Finally, the last phase of the Andes uplift, called Diaguita, ended about 3 Mya (Pliocene; Ortiz-Jaureguizar and Cladera, 2006) reaching the current altitude of the summits. Besides these vicariant effects determined by genetic barriers in different time periods, the orogenic process intensified the formation of corridors and valleys, building new habitats with their own microclimatic characteristics available for the diversification of several organisms (Linder, 2008; Graham, 2009; Renny et al., 2017), and particularly in plant genera, such as *Chuquiraga* (Ezcurra, 2002), *Calceolaria* (Cosacov et al., 2009), *Heliotropium* (Luebert et al., 2011), *Valeriana* (Bell et al., 2012), *Oxalis* (Heibl and Renner, 2012), *Nothofagus* (Acosta et al., 2014), and *Monttea* (Baranzelli et al., 2014, 2017).

The massive Andean mountain range affected organism lineages in different ways: as a genetic barrier, promoting disjunctions east and west of the Andes; as a corridor, fostering latitudinal genetic flow; and as promoter of new niches in high Andean ranges, generating new environments outside the mountain range (Luebert and Weigend, 2014 and references therein). Similarly important were the climatic changes occurred during the alternating glaciation cycles of the Pleistocene, which impacted on the distribution, diversification, and demographic dynamics of the southern South-American species (Sérsic et al., 2011). During the Pleistocene, several glaciations took place, with the Great Patagonian Glaciation (GPG, 1-1.2 Mya) and the Last Glacial Maximum (LGM, 20-18 Ka) being the most important (Coronato et al., 2004). During these glaciation periods, the climate became colder and drier, and concomitantly the sea level decreased and the coast line shifted to the east, exposing submerged areas, sometimes connecting islands to the mainland. For example, the Malvinas/Falkland Islands (hereafter Malvinas Islands) would have been connected to the mainland during GPG and LGM, favoring species interchange (Coronato et al., 2008). The effects of the Pleistocene glaciations affected not only the southernmost areas of Patagonia, but also the Andean regions of Peru and Bolivia, around 17°S, where glaciers were 1400 m lower than in the present (Seltzer, 1992; Clayton and Clapperton, 1997; Kull and Grosjean, 2000; Ammann et al., 2001; Mark et al., 2005).

To test the effects on diversification, distribution, and demography of the past orogenic processes and climatic changes occurred in southern South-America, we selected a plant species that presents current vicariant distribution along the Andean range. *Arachnitis uniflora* is a myco-heterotrophic plant species of the Corsiaceae family; it is a completely achlorophyllous geophyte that only becomes visible during the flowering and fruiting periods (Fig. 1, inset). Survival of this achlorophyllous species depends on an obligate association with arbuscular mycorrhizal fungi that are connected to green plants; the latter actually provide nutrients, conforming a tripartite relationship. Glomeraceae fungi were found to be dominant in this association (Bidartondo et al., 2002; Renny et al., 2017). Sexual reproduction in this species is poorly known (but, see Ibisch et al., 1996). The fruit is a capsule producing thousands of dust-like tiny seeds (Domínguez and Sérsic, 2004). *A. uniflora* presents a

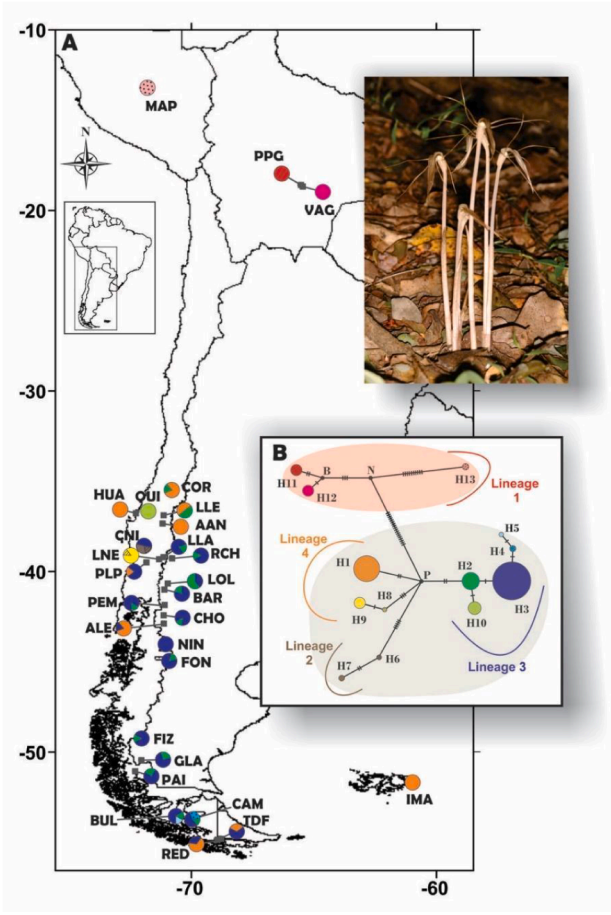

Fig. 1. Geographical distribution and genealogical relationship of the nuclear haplotypes in *Arachnitis uniflora*. (A) Map of southern South-America showing haplotype distribution. Pie charts indicate the haplotype frequency at each site. Site codes are indicated in Table 1. (B) Haplotype network. Each cross hatch between haplotypes represents one mutational step. Black dots (referenced as P, N, and B) represent extinct ancestors or missing intermediate haplotypes not found in the analysis. Colored areas represent the genetic groups retrieved by SAMOVA (i.e. Northern and Patagonian groups). Lineages correspond with those of the phylogenetic tree in Fig. 5. The insets depict the map of South America indicating the study area (left), and a photograph of *A. uniflora* flowering shoots (right).

particular disjunct distribution occurring in three very distant locations, mainly in the Andean–Patagonian temperate forests of Argentina and Chile; in the tropical semi-humid, mostly deciduous forests of Peru and Bolivia; and in the moorlands of Malvinas Islands (Dimitri, 1972; Graf, 1992; Ibisch et al., 1996; Ochoa et al., 2019). Ibisch et al. (1996) according to biogeographic data postulated that in the past there was a continuous distribution range between the southern and northern current distribution locations that became separated after the quaternary climatic changes. These disjunct areas are separated by vast and arid ecoregions not suitable for *Arachnitis*, such as Atacama Desert, Monte ecoregion, and the Patagonian steppe. Thus, although *Arachnitis* seed features could be concordant with a long-distance dispersal, this is considered unlikely (Ibisch et al., 1996).

Thus, this widely distributed and disjunct species offers the opportunity to explore the dynamics of evolutionary processes using phylogeographic approaches, and spatio-temporal and paleodistribution reconstructions. The first question that arises is if this disjunction is the result of a vicariance process or of long-distance dispersal. According to Ibisch et al. (1996) we hypothesize that in the past, *Arachnitis uniflora* was distributed more continuously from Peru to Patagonia. However, we consider that the orogenic processes and climatic changes occurred

during the Andean uplift would have mostly impacted in the fragmentation of the species distribution. We expect to find that the genetic diversity patterns of *A. uniflora* related to a vicariance process are concomitant with ancient geological events and climate changes occurred in the Miocene-Pliocene, whereas more recent Pleistocene events would have also impacted on species diversification, as inferred by Ibisch et al. (1996).

2. Materials and methods

2.1. Sampling

We collected plant tissues from 1 to 7 individuals from *A. uniflora* at 28 locations distributed throughout the entire geographical range in southern South-America (Table 1). Samples were dried in silica gel and stored until use. Voucher specimens were deposited in the herbarium of the Botanical Museum of Córdoba, Argentina (CORD). The outgroups were sequences of *Corsia* sp. (Corsiaceae) and *Burmannia bicolor* (Burmanniaceae); see Supplemental information Table S1.

2.2. DNA extraction, amplification, and sequencing

We extracted total genomic DNA following Wilkie (1997) and tested a total of 25 pairs of primers to assess intraspecific variation (8 mitochondrial, 9 chloroplast and 8 nuclear primers; Table S2). The most informative markers were three fragments of a nuclear DNA region and one of the chloroplast DNA. We used Sanger sequencing to amplify the complete internal transcribed spacer (ITS) region (including the 5.8S rRNA gene), 18S rRNA gene, and 26S rRNA gene using the primers ATGGTCCGGTGAAGTGTTCG (Sun et al., 1994) / TCCTCCGCTTATTGATATGC (White et al., 1990), GTAGTCATATGCTTGTCTC / CTTCCGTCAATTCCTTTAAG (White et al., 1990), and CGACCCCAGGTCAGGCG / GCTATCCTGAGGGAAACTTC (Kuzoff et al., 1998), respectively. In addition, we amplified one coding region of the chloroplast genome (16S rRNA gene) using the primers GGAGAGTTCGATCCTGGCTCAG / AAGGAGGTGATCCAGCC (Nickrent et al., 1997). Our decision of using Sanger sequencing arise in the need of analyse the evolution of discrete loci in multiple individuals to infer haplotype genealogies and phylogenetic trees, controlling what regions of the genome were sequenced (see McCormack et al., 2013).

The PCR mix contained 2.5 mM $MgCl_2$; 5 μL of buffer 10× [75 mM Tris-HCl pH 8.8; 20 mM $(NH_4)SO_4$; 0.01% Tween-20]; 200 μM of each nucleotide (dATP, dGTP, dCTP, dTTP); 0.2 μM of each primer; 1 unit of Taq DNA polymerase (Invitrogen, Brazil), and 10-15 ng of template DNA. The PCR cycling scheme was 5 min at 80 °C; 30 cycles of 1 min at 54 °C, 40 s at 50 °C (with 0.3 °C/ s ramp), and 4 min at 65 °C; a 5-min final extension at 65 °C, and a final hold at 15 °C. Amplification products were separated by electrophoresis on a 1% agarose gel, stained with Sybr Safe (Invitrogen, Eugene, OR, USA), and visualized with a blue light transilluminator. The PCR-amplified products were sequenced by Macrogen (Inc.). Sequences were aligned using MEGA v.6.0 (Tamura et al., 2013), with manual adjustments made as needed. Three nuclear regions were concatenated for each individual and were used as a unity.

2.3. Haplotype genealogy and population genetic diversity and structure

To examine genetic relationships among the haplotypes defined by DnaSP v.6.11.01 (Rozas et al., 2003), we constructed a median-joining network using NETWORK v.4.1.1.2 (Bandelt et al., 1999). Ambiguous connections (loops) in the network were resolved using predictions from

Table 1
Identification codes (ID) of collection sites of *Arachnitis uniflora* (A, Argentina; B, Bolivia; C, Chile; P, Peru), latitude, longitude, altitude, number of samples (N), polymorphic sites (S), genetic diversity indices (π and H), and haplotypes for each site, with both types of markers. *Estimated geographic position.

					Nuclear DNA					Plastid DNA				
ID	Site	Latitude	Longitude	Altitude	N	S	π	H	Haplotypes	N	S	π	H	Haplotypes
MAP	Machu Pichu (P)	−13.2	−72.5	2910	2	0	0	0	H13	1	–	–	–	H13
VAG	Valle Grande (B)	−18.6	−64.0	2387	6	0	0	0	H12	1	–	–	–	H12
PPG	Pampa Grande (B)	−18.7	−63.9	2378	6	0	0	0	H11	3	5	0.00277	1	H9-H11
COR	Corel (C)	−35.5	−71.2	487	5	3	0.00046	0.4	H1, H2	3	1	0.00055	0.667	H1, H6
QUI	Quillón (C)	−36.7	−72.5	41	7	0	0	0	H10	6	0	0	0	H1
HUA	Hualpén (C)	−36.8	−73.2	18	7	0	0	0	H1	5	0	0	0	H1
LLE	Los Lleuques (C)	−36.9	−71.6	730	2	3	0.00115	1	H1, H2	2	0	0	0	H1
AAN	Alto Antuco (C)	−37.4	−71.7	749	7	0	0	0	H1	5	1	0.0005	0.6	H1, H5
CNI	Ñielol Hill (C)	−38.7	−72.6	218	6	9	0.00203	0.733	H3, H6, H7	1	–	–	–	H1
LLA	Llancalil (C)	−39.2	−71.6	333	5	1	0.00015	0.4	H2, H3	5	3	0.001	0.7	H1, H2, H4
RCH	Ruca Choroy Lake (A)	−39.2	−71.2	1242	6	1	0.00013	0.333	H2, H3	5	2	0.00067	0.4	H1, H8
LNE	Los Nevados (C)	−39.3	−71.8	400	7	0	0	0	H8, H9	6	2	0.00072	0.733	H1-H3
PLP	La Peña (C)	−39.5	−72.6	154	5	4	0.00062	0.4	H1, H3	2	1	0.00062	1	H1, H7
LOL	Lolog Lake (A)	−40.7	−71.4	937	5	1	0.00023	0.6	H2, H3	5	1	0.0005	0.6	H1, H2, H4
BAR	San Carlos de Bariloche (A)	−41.1	−71.5	822	5	1	0.00015	0.4	H2, H3	2	0	0	0	H1
PEM	Perito Moreno Hill, El Bolsón (A)	−41.9	−71.5	593	6	1	0.00013	0.333	H2, H3	5	0	0	0	H1
CHO	Cholila (A)	−42.5	−71.6	580	7	1	0.00011	0.286	H2, H3	4	0	0	0	H1
ALE	Los Alerces National Park (A)	−42.9	−71.6	526	5	4	0.00062	0.4	H1, H3	4	0	0	0	H1
NIN	Los Niños Lagoon (A)	−44.0	−71.5	1026	2	0	0	0	H2, H3	1	x	x	x	H1
FON	Fontana Lake (A)	−44.9	−71.5	928	6	1	0.00013	0.333	H2, H3	2	0	0	0	H1
FIZ	Fitz Roy, El Chaltén (A)	−49.3	−72.9	693	6	1	0.00013	0.333	H2, H3	4	0	0	0	H1
GLA	Los Glaciares National Park (A)	−50.5	−72.9	403	4	1	0.00019	0.5	H2, H3	2	0	0	0	H1
PAI	Torres del Paine National Park (C)	−51.1	−73.2	258	4	1	0.00019	0.5	H2, H3	5	0	0	0	H1
IMA	Malvinas Islands (A)	−51.7*	−57.9*	–	1	–	–	–	H1	1	–	–	–	H1
BUL	Fuerte Bulnes (C)	−53.6	−70.9	404	6	2	0.00033	0.6	H2, H3, H5	2	0	0	0	H1
CAM	Puerto Cameron (C)	−53.7	−70.1	116	7	2	0.00029	0.667	H2-H5	3	0	0	0	H1
TDF	Tierra del Fuego National Park (A)	−54.8	−68.5	9	3	1	0.00026	0.667	H1, H3	3	0	0	0	H1
RED	Redonda Island (A)	−54.9	−68.5	402	3	4	0.00103	0.667	H1, H3	2	0	0	0	H1
Species					141	49	0.00215	0.746	H1-H13	90	28	0.00144	0.39	H1-H13

coalescent theory (Crandall and Templeton, 1993). Patterns of genetic diversity and structure were estimated by genetic landscape shape interpolation analyses using the program Alleles In Space v.1.0 (Miller, 2005). This procedure provides a graphical representation of inter-individual genetic distance that allows us to detect the location of putative barriers or contact zones with dissimilar gene composition. The analysis was carried out with a grid size of 50 × 50 and a distance weight value of a = 1 as suggested by Miller (2005).

To map the spatial distribution of genetic diversity, we performed interpolations with the haplotype diversity values (H), obtained for each location and each marker projected onto the modelled current distribution of *A. uniflora*, using the inverse distance weighting spatial interpolation method (IDW) in QGIS v.2.18 (QGIS Development Team, http://www.qgis.org/).

Groups of populations were identified with a spatial analysis of molecular variance, with and without constraint for the geographical composition of the groups, implemented in SAMOVA v.2.0 (Dupanloup et al., 2002). Analyses were run to evaluate different numbers of groups (K) ranging from K = 2 to 20 based on 100 simulated annealing steps. We selected the best clustering for each K value, based on the among-group component (FCT) of the overall genetic variance.

2.4. Molecular diversity indices and demographic analyses

We calculated haplotype diversity (Nei, 1987), nucleotide diversity (π; Nei, 1987) and number of polymorphic sites (S) for the species, for each location, and for every significant haplogroup derived from SAMOVA, using DnaSP. A mismatch distribution analysis was performed to distinguish models of past exponential growth versus historical population stasis (Rogers and Harpending, 1992; Excoffier, 2004). A multimodal distribution of differences between haplotypes is usually found in samples taken from populations at demographic equilibrium, whereas the distribution is usually unimodal in populations that have passed through a recent demographic expansion (Excoffier, 2004). The goodness-of-fit of the observed mismatch distribution to that expected under a sudden expansion model was evaluated using parametric bootstrapping with the sum of squared deviations (SSD). A significant SSD ($P \leq 0.05$) indicates deviation from the null model of population expansion. In addition, Tajima's D (Tajima, 1989) and Fu's F_s (Fu, 1997) tests of neutrality were performed to detect range expansions. Significant negative values of Tajima's D and Fu's F_S indicate population expansion. The significance of both values was calculated from 1000 simulated samples using a coalescent algorithm. Neutrality tests and mismatch distribution analyses were performed using ARLEQUIN v.3.1 (Excoffier et al., 2005), and the latter were graphed in DnaSP.

We used Bayesian Skyline Plot analysis (BSP; Drummond et al., 2005), implemented in BEAST v.1.6.2 (Drummond and Rambaut, 2007) to test changes in effective population size and the time of the beginning of an expansion in those SAMOVA groups that showed signals of expansion with the previous demographic analyses. The analysis was implemented using the optimal substitution model obtained by MRMODELTEST v.2.2 (Nylander, 2004) and a relaxed clock with a uniform-distributed prior clock rate. Root height and the clock mean rate were set according to the chronogram obtained with BEAST (see below). A randomly generated tree was used as the starting tree with a coalescent Bayesian Skyline tree prior consisting of ten groups and a piecewise-constant skyline model. The MCMC was run for 50 million generations, sampling every 1000 generations. The BSP was produced in TRACER v.1.5 (available from the BEAST site) using the log file from the analysis in BEAST and discarding 10% of the runs as burn-in.

2.5. Phylogenetic relationships among haplotypes and molecular dating

To estimate the haplotype divergences, we used sequences of 5.8S, 18S, and 26S rRNA regions of the following outgroups obtained from GenBank: *Alstroemeria* spp., *Burmannia* spp., *Campynema lineare*, *Colchicum* spp., *Corsia* spp., *Lapageria rosea*, *Lilium* spp., *Luzuriaga radicans*, *Ripogonum elseyanum*, *Smilax* spp., *Trillium* spp., and *Veratrum nigrum* (see GenBank accession numbers in Table S1). First, a phylogeny of Liliales was constructed using a Bayesian analysis in MRBAYES v.3.1.2 (Ronquist and Huelsenbeck, 2003) with a model of sequence evolution generated by MRMODELTEST that implemented the hierarchical likelihood ratio test (hLRT) and the Akaike Information Criterion (AIC). The evolution model that best fit nuclear datasets was GTR + I + G (Rodríguez et al., 1990). The analysis consisted of two independent runs of 4×10^6 generations with four chains each (three heated and one cold) and trees were saved every 100 generations in each run. Approximately 10% of the trees (corresponding to the burn-in period) were discarded and a 50% majority rule consensus tree was constructed from the remaining trees (Fig. S1).

We estimate divergence times using BEAST, preparing the input file in BEAUti v.1.6.2 (provided in the BEAST package). The substitution model was GTR + I + G with a Gamma site heterogeneity model with four categories following the MRMODELTEST result; the clock was set as an uncorrelated lognormal relaxed model, and the Yule process was selected as a prior for the distribution of divergence dates. We set the Monte Carlo Markov Chain to run for 2×10^7 generations, sampling every 1000 cycles.

We considered the split of Liliales and *Burmania* as the root of the tree, setting it to 110 Mya (±10 Mya) with normal distribution. Additional time constraints were set for the crown of Liliales at 85 Mya, the split of *Alstroemeria* from *Luzuriaga* (uniform distribution; lower: 21.5 Mya; upper: 80 Mya), and *Lapageria* and *Ripogonum* (uniform distribution; lower: 51 Mya; upper: 80 Mya); we took all these dates from Mennes et al. (2015). Then, we used the resulting chronology (Fig. S1) to indirectly obtain the ages of the split between *Corsia* and *Arachnitis*, and the diversification date of *Arachnitis*. We employed these ages as secondary calibration points in the molecular dating of *Arachnitis* phylogeny with the complete nuclear and chloroplast data. The evolution models selected were GTR and GTR + G for nuclear and chloroplast data, respectively. We set the Monte Carlo Markov Chain to run for 5×10^7 generations, with sampling every 1000 cycles.

2.6. Bayesian spatio-temporal diffusion analyses

We reconstructed the evolutionary history of the species in space and time assuming continuous spatial diffusion, using a time-heterogeneous random walk model (Relaxed Random Walk; RRW; Lemey et al., 2010) in BEAST. We ran two independent analyses using pDNA and nDNA matrices, which included one individual per haplotype per locality. According to the Akaike Information Criterion (AIC) implemented in jModelTest v.2.0.2 (Darriba et al., 2012), the best-fit mutation models selected were HKY + I for both matrices. We used a lognormal relaxed clock, and a coalescent Bayesian Skyride model; as priors, we used the mutation rates obtained with dating analyses (see above), i.e. 0.0005075 substitutions per site per million years for nDNA and 0.000635 substitutions per site per million years for pDNA. As rootHeight we selected the beginning of *A. uniflora* diversification obtained with the molecular dating analyses, using a normal distribution (7.4 ± 2, for nDNA and 8.37 ± 2 for pDNA). The length of MCMC was 1×10^9 generations for both runs, which is the necessary length to obtain 10,000 trees. To summarize the posterior distribution of ancestral ranges using the RRW model, we annotated nodes in a maximum clade credibility tree (MCC) using TreeAnnotator v.1.7.5. This tree was then used as an input in SPREAD v.1.0.7 (Bielejec et al., 2011) to reconstruct the spatial diffusion pattern, and was viewed using Google Earth (http://earth.google.com).

2.7. Species paleo-distribution range

To detect possible shifts in the species distribution we performed paleo-distribution modelling under different climatic scenarios using the

28 *A. uniflora* sites georeferenced in the field, and reliable coordinates obtained from several Herbaria databases (CONC, IS) or from the literature. We obtained a total of 51 points after eliminating redundant or too close georeferences. We calibrated the model manually by randomly selecting 65% of the clean occurrence dataset for calibration and 35% for validation. We estimated the area M, i.e., the area that was accessible to the species through dispersal over relevant time periods, as the area for calibrating the model (Soberón and Peterson, 2005; Soberón, 2007; Barve et al., 2011). We downloaded the 19 bioclimatic layers from the PaleoClim dataset (http://www.paleoclim.org/) for current conditions (~1979–2013; 2.5 arcmin. CHELSA); we searched for correlations between the bioclimatic variables and selected those variables that were not correlated (Pearson $\geq$ 0.85; Osorio-Olvera et al., 2016); thus, we retained the following variables: Annual mean temperature (Bio1), Mean diurnal range (Bio2), Isothermallity (Bio3), Temperature seasonality (Bio4), Max Temperature of Warmest Month (Bio5), Temperature Annual Range (Bio7), Mean Temperature of Wettest Quarter (Bio8), Annual precipitation (Bio12), Precipitation of the driest month (Bio14) and Precipitation of the warmer quarter (Bio18). We tested nine different algorithms for the current distribution model: Bioclim (Busby, 1991), Domain (Carpenter et al., 1993), GLM (Guisan et al., 2002), Rforest (Liaw and Wiener, 2002), SVM (Karatzoglou et al., 2004), Mahalanobis (Farber and Kadmon, 2003; see Supplemental Material S1), and three selected (LQHPT_3, LQHP_3, LQHP_2) MaxEnt models (Phillips et al., 2006). To select these three MaxEnt models, a total of 48 models were evaluated with R package ENMeval (Muscarella et al., 2017) to test a set of predictor variables (i.e. feature classes, Fc) together with different multiplier regularization (Rm) values; of all models, the first three with the lowest AICc values and the lowest omission rates were chosen. The nine current models were validated in Niche ToolBox (Osorio-Olvera et al., 2016) using 35% of the presence points and 14 additional absence points. For validation, we tested the partial-ROC values (Peterson et al., 2008) and those tests that depend on the threshold: binomial test (Anderson et al., 2002), True Skill Statistic (TSS; Allouche et al., 2006), Kappa (Cohen, 1960), prevalence (proportion of presences respect to total presence and absence points), sensitivity (probability that a point of presence was correctly predicted), omission error (false negative; Fielding and Bell, 1997), commission error (predicted present but actually absent), following Camps et al. (2018). The selected threshold values were the minimum training presence (Supplemental Material S1).

The selected current model was projected to the Last Glacial Maximum (LGM; ~21 Kya; 2.5 arcmin), Last Interglacial Maximum (LIG, ~116–130 Kya; 2.5 arcmin), and Marine Isotope Stage 19 (MIS19; ~787 Kyr; 2.5 arcmin) climatic scenarios downloaded from the PaleoClim database (http://www.paleoclim.org; Brown et al., 2018). Since some layers are not available for MIS19, we worked with Bio1, Bio4, Bio8, Bio12, Bio14 and Bio18. For the LGM, we used two Global Climate Models, CCSM and MIROC.

We reprojected the current and past distribution models obtained onto maps using the minimum training presence threshold as the lowest probability value of favorable area for the species. We averaged CCSM and MIROC LGM projections to obtain the final projection.

3. Results

Nuclear DNA regions were sequenced in a total of 141 *A. uniflora* individuals from 28 localities. Nuclear fragments belonging to 18S, ITS and 26S regions were concatenated and treated as a unit, resulting in 2604 pb (see GenBank accession numbers in Table S3). The whole nuclear sequences showed 49 informative sites, with a nucleotide diversity of $\pi = 0.00215$. The localities with the highest diversity were CNI, LLE and RED, with π values higher than 0.001 (Table 1). Chloroplast DNA (16S) was sequenced in a total of 90 *A. uniflora* individuals from 28 localities (see GenBank accession numbers in Table S3). Twenty-eight informative sites were detected along the 1207 pb region; nucleotide diversity was $\pi = 0.00144$. Localities PPG, LLA, PLP, LNE, RCH, COR, AAN, and LOL were the only ones with nucleotide diversity values higher than 0; PPG represented the highest diversity, and together with LLA, both evidenced π values higher than 0.001 (Table 1).

3.1. Haplotypes genealogy

Nuclear sequences resulted in 13 haplotypes, with a haplotype diversity of H = 0.746, and with LLE, CNI, RED, CAM, and TDF sites achieving diversity values higher than 0.65 (Table 1). The nuclear haplotype network (Fig. 1) displayed H3 as the most frequent haplotype, whereas H1 was the most widely distributed at the extremes of Patagonia, and Malvinas Islands. The second most frequent haplotype was H2, which occupied a high number of sites along the Patagonian forest. The remaining haplotypes were exclusive to several populations. The haplotype network revealed two genetic groups, a northern group (Bolivia and Peru, hereafter, Northern group) and a southern group (hereafter, Patagonian group) separated by 18 mutational steps. Chloroplast DNA sequences amounted to 13 haplotypes, accounting for a haplotype diversity of H = 0.39. Only at sites PLP, PPG, LNE, LLA, COR, AAN, LOL, and RCH was haplotype diversity higher than 0 (Table 1). Haplotype network (Fig. 2) also showed a divergence of two haplogroups separated by 12 mutational steps. The Northern group includes the Bolivian and Peruvian sites, with all haplotypes being exclusive. The Patagonian group evidenced the typical star-like topology, with a most frequent central haplotype (H1), which was present in all Andean-Patagonian sites and in Malvinas Islands. Except for H2, all haplotypes derived from H1 were exclusive to sites located in the northern distribution range of Patagonia.

3.2. Geographic distribution of genetic diversity

Genetic landscape shape interpolation analyses performed with Andean-Patagonian forest localities of *A. uniflora* showed the highest values of nucleotide diversity (i.e. dissimilar sequences in a short geographic distance, graphed as ascendant or positive peaks) at 39.4°S (between LNE and PLP), which was revealed with nDNA and pDNA data (Fig. 3). Another evident peak was found at about 44.5°S (near FON) with both DNA datasets.

Interpolation of haplotype diversity of *A. uniflora* was useful to infer the geographical distribution of genetic diversity (Fig. 4). The spatial mapping of nDNA and pDNA genetic diversity showed two genetic hot spots north of 40°S latitude. In addition, the highest nDNA haplotype diversity values were found in the southernmost areas of Patagonia. Northern group evidenced low haplotype diversity with nDNA. However, the maximum of pDNA genetic diversity was evidenced in Bolivia.

3.3. Population structuring

The best configuration of population clustering performed with SAMOVA evidenced K = 2 groups, in both types of DNA datasets. The optimal partitioning of nuclear and chloroplast DNA genetic diversity inferred from SAMOVA was obtained with K = 2 with (FCT = 0.872; $P <$ 0.0000; FCT = 0.942; $P < 0.001$, respectively) and without (FCT = 0.872; P < 0.0000; FCT = 0.942; P < 0.000) constraints for the geographical composition of the groups. Analyses for the remaining K values generated single population groupings, although the differences among the groups were maximized. Thus, two genealogically well-defined genetic populations were recognized: a Northern group, including Bolivian and Peruvian localities, and a Patagonian group, comprising all Andean-Patagonian sites, including Malvinas Island sample.

3.4. Phylogenetic analyses

Phylogeny of Liliales, including *A. uniflora* sequences (Fig. S1), was

1

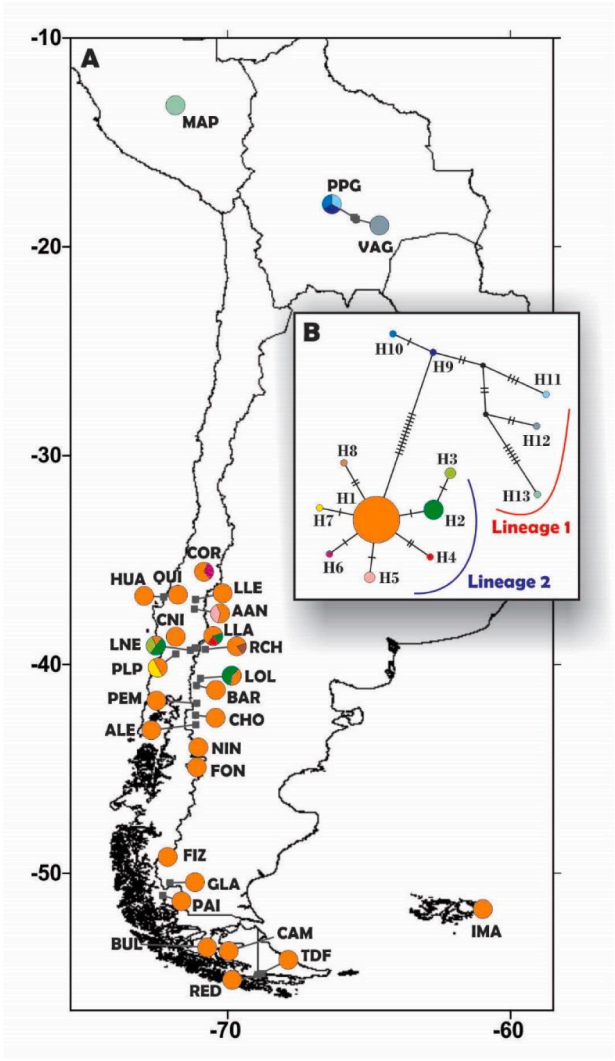

Fig. 2. Geographical distribution and genealogical relationship of the chloroplast haplotypes in *Arachnitis uniflora*. (A) Map of southern South-America showing haplotype distribution. Pie charts indicate the haplotype frequency at each site. Site codes are indicated in Table 1. (B) Haplotype network. Each cross hatch between haplotypes represents one mutational step. Black dots represent extinct ancestors or missing intermediate haplotypes not found in the analysis. Colored areas represent the genetic groups retrieved by SAMOVA (i.e. Northern and Patagonian groups). The inset depicts the map of South America indicating the study area.

reconstructed with Bayesian inference. Support of nodes was relatively high, except for Corsiaceae clade, which evidenced a low Bayesian Posterior Probability (BPP = 0.54). The age obtained for the divergence between *Corsia* and *Arachnitis* was estimated in 48.6 Mya (Fig. S1). The first divergence within current *A. uniflora* haplotypes occurred in the late Miocene, about 8.4 - 7.5 Mya (Bayesian Posterior Probability, BPP = 1.00), with the split between Northern (Bolivian and Peruvian sites) and Patagonian (including Malvinas Islands) groups (Fig. 5). Posterior diversification of *A. uniflora* allowed grouping of haplotypes into lineages in correlation with the respective haplotype networks. The beginning of diversification in Andean-Patagonian haplotypes was dated to about the end of the Miocene and the beginning of the Pliocene, between 5.5 and 4.1 Mya (BPPs = 0.88 and 0.91), whereas the emergence of current haplotypes occurred in the Mid-Pleistocene, between 1.2 and 0.4 Mya (BPP higher than 0.91). Haplotypes belonging to Bolivian and Peruvian distribution of *A. uniflora* started their diversification in the Pliocene, about 5.2 to 3.5 Mya (BPP = 0.96 and 1.00). The last divergences were dated in the early-middle Pleistocene, between 2.1 and 1.2 Mya. Confidence intervals of the main dated nodes are summarized in Table S4.

3.5. Past demographic processes

All the neutrality tests performed according to the genetic groups obtained by SAMOVA resulted non-significant for the Northern group ($p > 0.05$; Table 2). On the one hand, Patagonian group evidenced a significant demographic expansion signal ($p < 0.002$) with pDNA, where D = −1.95126, and Fs = −6.21434; however, nDNA evidence resulted non-significant ($p > 0.4$) for demographic expansion. Similarly, mismatch distribution analyses (Fig. S2) showed multimodal distributions for Northern group, whereas in Patagonian group it was unimodal only with plastid sequences (Fig. S2D), evidencing demographic expansion. However, Sum of Squared Deviation (SSD) was (i.e. both genetic groups and both kinds of DNA evidence) non-significant in all cases, being in disagreement with its corresponding multimodal graphs for Northern group (Figs. S2A and S2C) and nuclear-defined Patagonian group (Fig. S2B). Patagonian group showed SSD = 0.00056 ($p = 0.6680$) values (with pDNA evidence), which is consistent with a recent demographic expansion.

Bayesian skyline plot (BSP) analysis was performed only for Patagonian group using the chloroplast evidence, because only in this group were the neutrality test values and mismatch analysis in agreement with a recent demographic expansion. This BSP graph shows that demographic growth started ca. 2.5-2 Mya (Fig. 5C).

3.6. Spatio-temporal diffusion analyses

Both molecular markers showed similar patterns in the diffusion analysis results, although they differ slightly in the dating; both analyses showed uncertainty in relation to the common ancestral area, placing the first divergence always further north than the northernmost Patagonian distribution. Current distribution areas were already colonized between 5 and 2 Mya, showing a first disjunction between the northern (Bolivia and Peru) and Patagonian areas of the species distribution. Divergence between Peruvian and Bolivian lineages in the Northern group occurred before the GPG (Supplemental Videos S1 and S2). Within the Patagonian distribution, both markers showed a relatively old colonization from northern to southern Patagonia before the GPG. Recent colonizations occurred between the GPG and the LIG, and were detected at several points in the central-northern and southernmost areas of the Patagonian distribution. The lineage that colonized Malvinas Islands diverged at 1 Mya and arrived at around 350 Kya with the nDNA, whereas in the pDNA it started at around 2.7 Mya and ended at 600 Kya (Fig. 6).

3.7. Species Paleo-distribution range

Ten bioclimatic variables were not correlated (<0.85); permutation importance values are summarized in Supplemental Material S1. The variables that most contributed to the determination of the current potential distribution of *A. uniflora* were Annual precipitation (Bio12), Precipitation of the driest month (Bio14), Mean temperature of wettest quarter (Bio8), and Precipitation of the warmer quarter (Bio18). For the current *A. uniflora* climatic conditions, we selected MaxEnt algorithm (Fc: LQHPT; Rm: 3), because it presented the best values of AUC and partial ROC, based on the threshold dependent metrics; additionally, it has highest values of Kappa and TSS metrics, low omission (although shared with other models) and a low value commission error (see Supplemental Material S1).

All species distribution models showed similar patterns from the MIS (787 Kyr) to the present. Projected areas showed the current disjunction between Northern and Patagonian groups for all past climatic scenarios (Fig. 7). The predicted area of the Northern group is a continuous strip

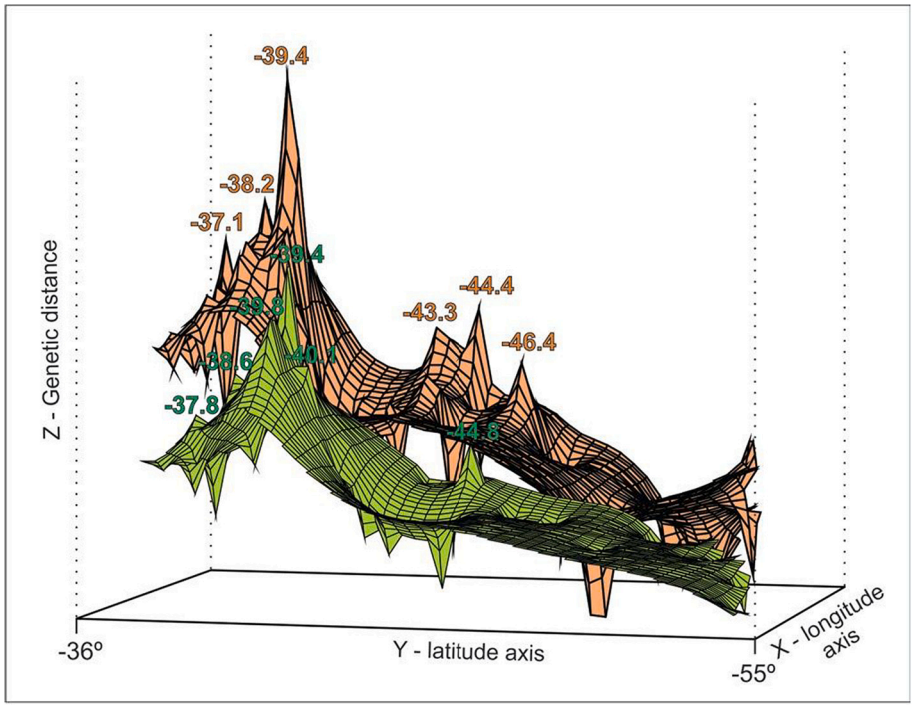

Fig. 3. Genetic landscape shape interpolation analysis using a 50 × 50 grid size and a distance weighting parameter of a = 1. The X- and Y-axes correspond to geographic locations; the *Z*-axis shows genetic distances. Positive peaks in relation to Z-axis show genetic discontinuities or possible barriers to gene flow, and are referenced with latitude coordinates. In orange, analysis performed with nDNA sequences, and in green with pDNA sequences of the Andean-Patagonian forest localities. (For interpretation of the references to colour in this figure legend, the reader is referred to the web version of this article.)

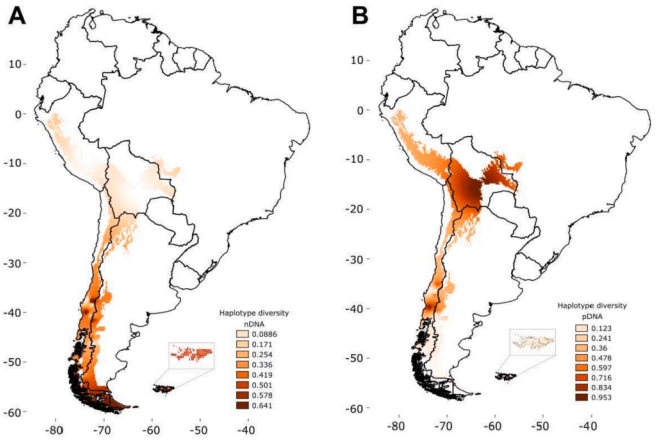

Fig. 4. Maps showing the Inverse Distance Weighting (IDW) spatial interpolation of haplotype diversity (H), performed with nDNA (A) and pDNA (B).

extending between Peru and Bolivia. The highest presence probability values and the largest occupied area were predicted for the LIG than for the other time periods. The Patagonian group also showed a continuum strip along the Andes from 35°S up to the southernmost areas of Tierra del Fuego. The highest probability values were detected mainly in the Andean-Patagonian forests, between 39°S and 49°S. The interglacial projection (LIG) showed that species distribution extended to the east in north Patagonia and predicted two coastal areas, with very low probability values of occurrence, at 40°S and 45°S (Fig. 7B). The LGM predicted a slight shift towards the east at approximately 35°S, and the species was also predicted on the marine platform southern than Tierra del Fuego, Los Estados Islands, the Burdwood Bank, and around Malvinas Islands (Fig. 7C).

4. Discussion

The development of molecular tools provides additional evidence for understanding the evolutionary relationships of plants (e.g. Chase et al., 1993). Mycoheterotrophic plants were not an exception in this revolution in the field of biology. Their peculiar *modus vivendi* offers several challenging issues. Molecular studies in this type of plant species have been performed at the interspecific level, with emphasis on phylogenetic and taxonomic perspectives (e.g. Lemaire et al., 2011; Merckx et al., 2013a; Mennes et al., 2015; Merckx et al., 2017); the only intraspecific approach was performed to unravel species delimitation among four related mycoheterotrophic orchid species (Barrett and Freudenstein, 2011). Our study is the first one referring to the evolutionary history of a mycoheterotrophic plant species in relation to historical, geological and climatic processes.

In order to elucidate the intraspecific relationship among distant populations of *A. uniflora*, we tested several chloroplast primers; many of them were not able to amplify genes associated with the photosynthetic pathway (see Table S2). As was reported for some achlorophyllous species (DePamphilis et al., 1997), the plastid genome of *A. uniflora* has undergone an extreme reduction in gene content and an increase in evolutionary rate of the remaining genes. *A. uniflora* has the smallest plastid genome of all plastids from Liliales sequenced by Do et al. (2020). The genes retained in *A. uniflora* show that plastids have other essential functions besides photosynthesis, since photosynthesis-related genes were deleted or pseudogenized, whereas genes of ribosomal proteins, rRNAs (such as the one sequenced in this work), and some tRNAs remained intact (Do et al., 2020). In addition, long branches of *A. uniflora* in comparison with related species evidence increased substitution rates in plastid genome, as was observed in the phylogeny provided by Mennes et al. (2015) and Do et al. (2020). We also found long branches in the nuclear DNA phylogeny, as reported for several achlorophyllous angiosperms (Lemaire et al., 2011). It would be enriching for future works to enlarge the molecular dataset with methodologies that explore the complete genome of the species.

4.1. Inference of spatio-temporal divergences of genetic diversity in *A. uniflora*

Ancient climatic changes and geological events clearly impacted on the spatial distribution of genetic diversity of *A. uniflora* over time, structuring the current distribution patterns. Phylogenetic analysis of

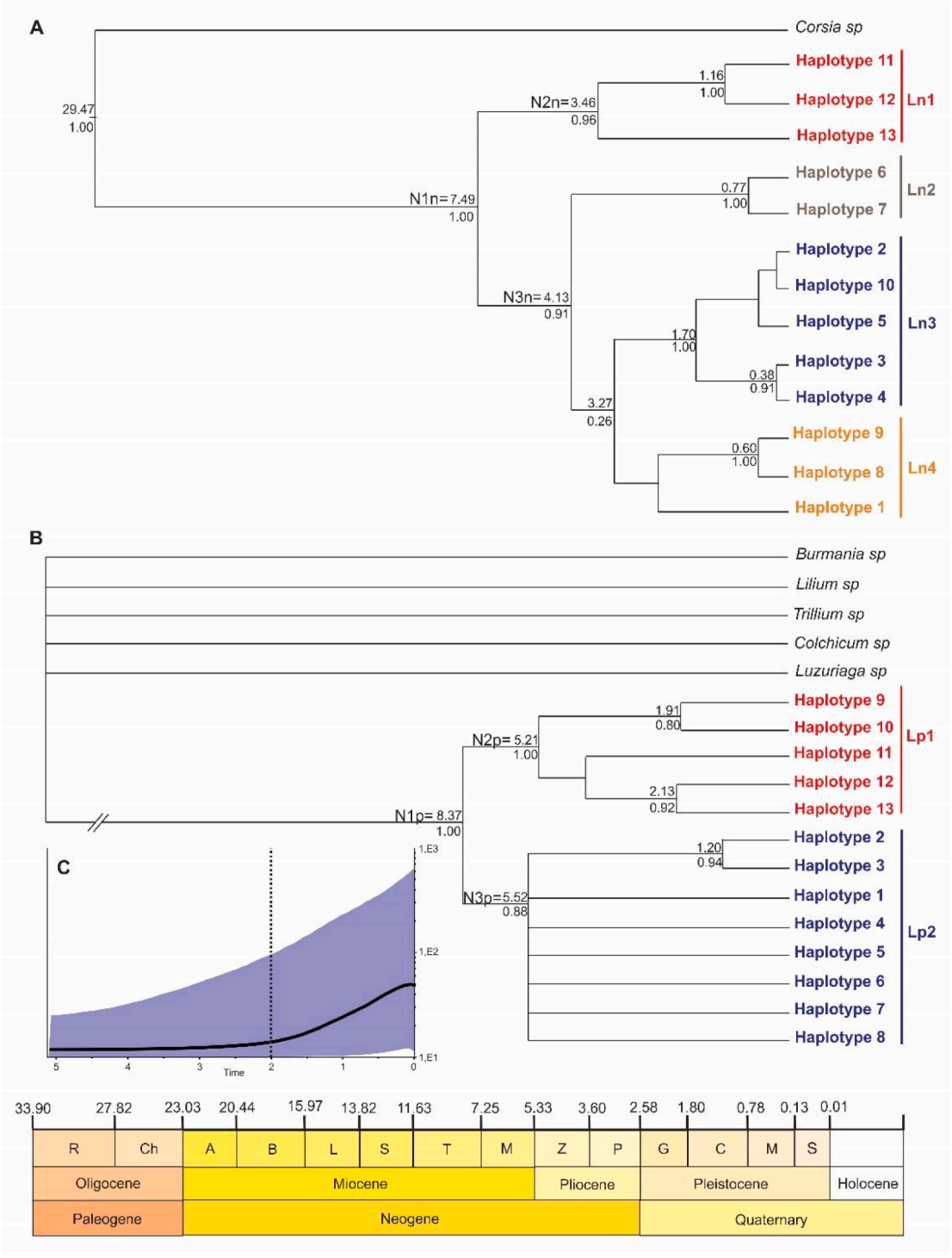

Fig. 5. Chronograms showing the evolutionary relationships among haplotypes of *Arachnitis uniflora* performed with nDNA (A) and pDNA (B). Numbers above branches indicate the age obtained from the molecular dating analysis (in Mya). Numbers below branches indicate the Bayesian posterior probability (BPP) values for Bayesian inference analyses. Lineages (L) are indicated with colors and correspond to the lineages of Figs. 1 and 2. Only supported nodes are referenced (except for the split between nuclear lineages Ln3 and Ln4, which is referred in main text). Trees are referenced with a timeline of International Chronostratigraphic Chart (2020; http://www.stratigraphy.org/ICSchart/ChronostratChart2020-01.pdf), which is shown at the bottom of the figure. The 95% confidence interval of main nodes are detailed in Table S4. Dashes ('//') indicate branches that are longer than indicated in the fig. (C) Bayesian Skyline Plot showing changes in effective population size over time (in Mya) for Patagonian group with pDNA.

the genus within the Liliales revealed an ancient origin of *Arachnitis* in the Upper Eocene (48 Mya), in agreement with Mennes et al. (2015). Merckx et al. (2013b) explained that high global temperatures during the Eocene provided a suitable environment, promoting mycoheterotrophic plant diversity in widely extended tropical rain forests at that time. In fact, *Arachnitis* also diversified in the Eocene, probably associated with woody species such as *Nothofagus*, *Araucaria* and *Podocarpus*, which were recorded at that time in Patagonia and persisted under cold temperatures, becoming part of the temperate forests (Romero, 1986; Barreda, 1996; Bidartondo et al., 2002; Panti, 2011; Palazzesi and

Table 2
Demographic results (Fs, D, and SSD) inferred for the genetic groups (Northern and Patagonian) retrieved by SAMOVA for *Arachnitis uniflora* for both types of markers. Number of samples (N), polymorphic sites (S), genetic diversity indices (π and H), and haplotypes. Significance values (p) are shown between parentheses. Values representing recent expansion in the effective population size are indicated in bold. *$p < 0.01$.

	Group	N	S	π	H	Haplotypes	D	Fs	SSD
Nuclear DNA	Northern	13	14	0.00127	0.615	H11-H133	0.07469 (0.490)	5.68372 (0.994)	**0.19245 (0.060)**
	Patagonian	128	41	0.00125	0.695	H1-H10	−0.24481 (0.404)	1.06864 (0.724)	**0.24200 (0.253)**
Plastid DNA	Northern	5	13	0.00522	1	H9-H13	0.06983 (0.4832)	−0.98743 (0.1898)	**0.01958 (0.8910)**
	Patagonian	85	9	0.00035	0.317	H1-H8	**−1.95126 (0.0017*)**	**−6.21434 (0.0001*)**	**0.00056 (0.6680)**

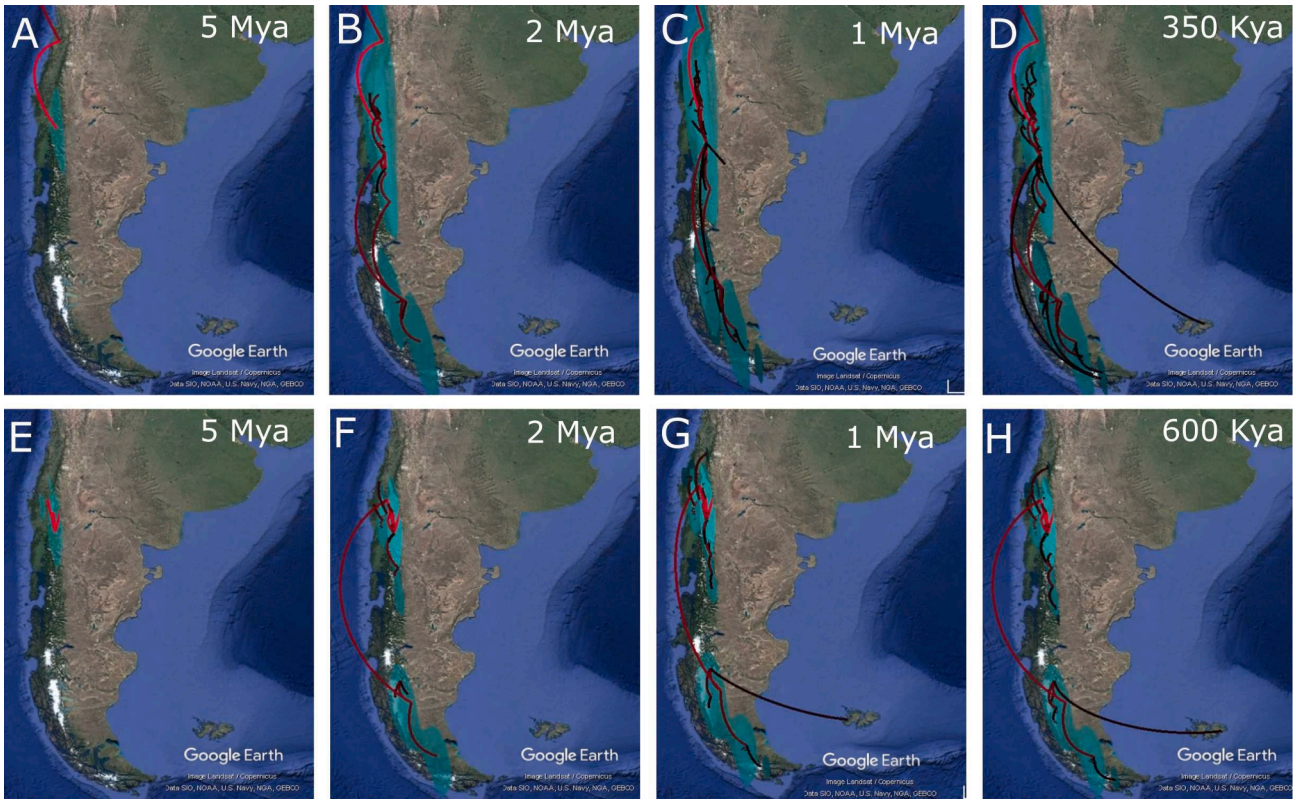

Fig. 6. Bayesian spatio-temporal diffusion analysis of *Arachnitis uniflora* nDNA (A-D) and pDNA (*E*-H) lineages at different time points, based on the maximum clade credibility (MCC) tree. Time slices are: 5 Mya (A and E), 2 Mya (B and F), 1 Mya (C and G), 600 Kya (H), and 350 Kya (D). Lines represent branches of the MCC tree; old lineages are in red, and recent lineages in black; shaded areas: 80%-HPD uncertainty in the location of ancestral branches, shading gradient indicates older (dark) versus younger (light) events. (For interpretation of the references to colour in this figure legend, the reader is referred to the web version of this article.)

Barreda, 2012; Wilf et al., 2013; Renny et al., 2017).

An ancient vicariance was revealed by the spatial distribution of haplotypes and network topology of both types of molecular markers. A long-lasting isolation of the two main haplogroups, the Northern and the Patagonian groups, was revealed by the absence of shared haplotypes and the presence of several mutational steps between them. This genetic divergence in the two main groups was also detected by SAMOVA and by the topology of the phylogenetic relationships performed with both markers. According to all these results, there is no evidence of long-distance dispersal, as suggested by Ibisch et al. (1996). Crown diversification of current haplotypes occurred during the Late Miocene (8.37 - 7.49 Mya), splitting the Northern and Patagonian groups. This period coincides with the Quechua phase, one of the last stages of the Andean uplift that provoked the rain shadow that gave rise to the Arid Diagonal (Hueck, 1978; Ortiz-Jaureguizar and Cladera, 2006; Ramos and Ghiglione, 2008). Villagrán and Hinojosa (1997) associated this event with the disruption of any posterior floristic interchange between Patagonia and the northern areas beyond the Arid diagonal. Additionally, Ezcurra (2002) proposed that, before the formation of the Arid Diagonal, the Andean uplift produced a continuum of cold climate from northern Patagonia towards the Central Andes. This corridor would have been effective for *A. uniflora* displacement only before the complete aridization. Andean orogeny could have had a twofold role in *A. uniflora* distribution, first as a dispersion corridor and then, as a barrier to humid Pacific winds, giving rise to the rain shadow.

Haplotype diversification of both main lineages (Northern and Patagonian groups) started during the transition from the Miocene to the early Pliocene. Patagonian group diversification started approximately 5.5 - 4.1 Mya, concomitantly with the cooling events recorded in South America due to the first glaciation episodes (7.4 - 5 Mya; Mörner and Sylwan, 1989; Ton-That et al., 1999; Ortiz-Jaureguizar and Cladera, 2006; Rabassa, 2008; Rabassa et al., 2011). During this period, Patagonia landscape also underwent fragmentation, due to marine transgressions (see Fig. 4d in Acosta et al., 2014). The first diversifications of the Northern group also occurred between 5.21 and 3.46 Mya, and were more related to the Andean uplift during the Diaguita phase than to the first glaciation events already mentioned. Successive posterior haplotype diversifications occurred between 2.13 and 1.16 Mya (split between Bolivia and Peru sites), which coincides with the cooling period that started in Bolivia between 2.7 and 1.6 Mya (Lavenu, 1986).

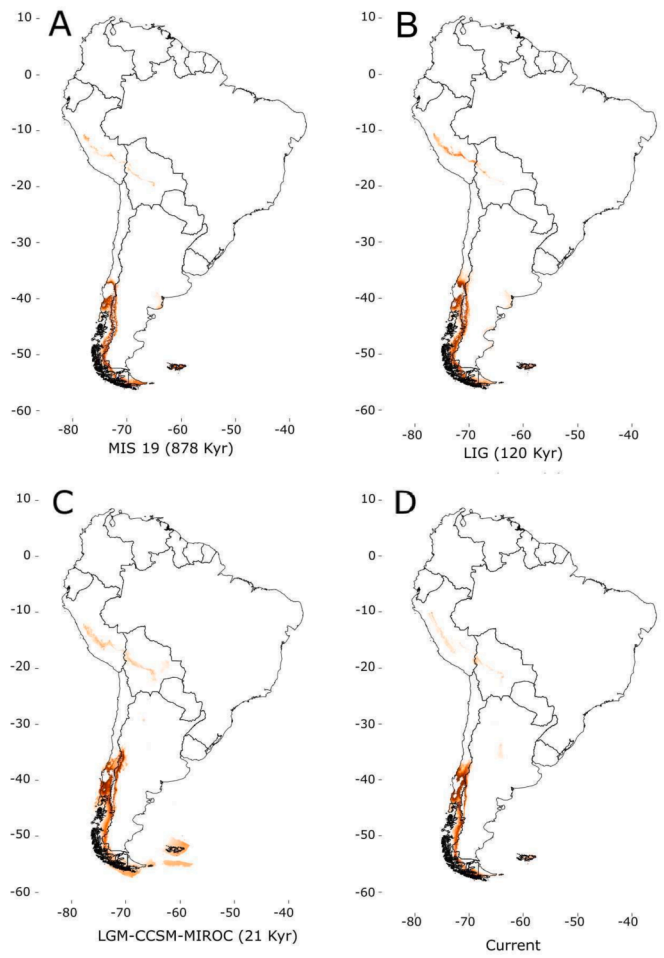

Fig. 7. Species distribution models of *Arachnitis uniflora* across Pleistocene climatic scenarios. (A) Last Glacial Maximum (LGM; ~21 Kya). (B) Last Interglacial Maximum (LIG; ~116–130 Kya). (C) Marine Isotope Stage 19 (MIS19; ~787 Kyr). (D) Present. Darker colors represent higher occurrence probability.

4.2. Pleistocene diversification into Patagonian group of A. uniflora

The large number of studied sites and the complex pattern of spatial genetic diversity in Patagonia allowed us to have a detailed panorama about the process of species colonization in several areas, and to infer the role of climatic and orogenic events. According to the molecular dating, the split of the two most frequent nDNA lineages (3 and 4) occurred in the early Pleistocene. In addition, the diffusion analysis allowed us to infer that these lineages originated in northern Patagonia and expanded independently towards the South. Results suggest that lineage 4 was decimated, persisting in sites located at the extreme areas of its distribution. On the other hand, lineage 3 colonized continuously southern areas up to Tierra del Fuego, where it persisted and diversified. As a contribution to the understanding of these dispersion episodes, we propose that the Andean landscape played an important role in shaping the demography of *A. uniflora*, acting as a corridor for species dispersion along the Andean Patagonian forest; this situation has been observed for other taxa at interspecific level (Linder, 2008; Luebert and Weigend, 2014; Bacon et al., 2018). In agreement with the diversification time of these nuclear lineages, diffusion analysis of the pDNA showed a similar colonization pattern, and the Bayesian Skyline Plot results evidenced a demographic expansion at approximately 2 Mya. Before the GPG, most lineages of both markers had arrived in the current species distribution range, and most diversifications had occurred. Only some recent diversifications occurred after GPG and long before the LGM, suggesting that LGM had a minor importance in molding genetic diversity patterns.

High genetic diversity and exclusive haplotypes revealed by spatial distribution of haplotypes and interpolation results showed the presence of several refugial areas. To the north of 37°-38°S in the Chilean coastal mountain, a lowland glacial refugium (QUI, COR, and AAN) was detected, and periglacial refugia in the Chilean Central Depression (PLP and CNI) and western side of the Andes (LNE and LLA). For this latitude, similar refugia were previously described by Sérsic et al. (2011) and Vergara et al. (2014). In correspondence with these refugial areas, a genetic break was detected at 39.4°S according to AIS results. This break is concordant with the barrier postulated for several species reported by Sérsic et al. (2011).

To the south of 40°S, genetic diversity of *A. uniflora* was clearly poor for both markers. Particularly, pDNA showed no variability at all, with all sites being monomorphic of the most frequent haplotype. By contrast, the nDNA showed a predominance of haplotypes of lineage 3, revealing a refugium with a high diversity area and exclusive haplotypes at the southernmost sites of the distribution in Tierra del Fuego. *A. uniflora* is a cold-tolerant species that probably survived in situ in southern South-America, as described by Souto and Premoli (2007) and Premoli et al. (2010) for *Embothrium coccineum* and *Nothofagus* species, and reviewed by Sérsic et al. (2011).

As a general outline, the genetic structure found for *A. uniflora* agrees with mapped genetic hotspots performed by Souto et al. (2015) for temperate forest tree species, with high diversity being concentrated around 40°S and in Tierra del Fuego, and with low genetic diversity at intermediate locations. Additionally, the four areas of high genetic diversity delimited in this work are remarkably coincident with high genetic diversity areas recorded for the main clade of arbuscular mycorrhizal fungi associated with *A. uniflora* (Renny et al., 2017): Bolivian sites; Chilean coastal mountain, around 36°S; Chilean Central Depression and western side of the Andes, near 39°S; and Tierra del Fuego island. Thus, genetic diversity of interacting species with similar geographical ranges would have been affected by common biogeographic processes (Souto et al., 2015).

Finally, the results obtained for *A. uniflora* in Malvinas islands may not reflect the complete scenario due to the scarcity of samples; in fact, both markers displayed the most frequent and widespread haplotypes, possibly introducing a bias in the interpretation of patterns. According to Coronato et al. (2008), a sea level drop of 150 m would be enough to connect the Malvinas Islands with the mainland. The paleo-distribution models showed that a possible path was formed during glacial periods, connecting the mainland with Malvinas Islands through Tierra del Fuego, Los Estados Islands, and the Burdwood Bank; however, due to the single sample we had from Malvinas Islands, diffusion analysis could not reconstruct this colonization route properly. Diffusion analysis estimated this connection during GPG, when the sea level may have dropped sufficiently to make this connection possible. Similar connections were recorded by Baranzelli et al. (2018) for the Lady slipper *Calceolaria fothergillii* and by Slater et al. (2009) for the Malvina's wolf (*Dusicyon australis*).

5. Concluding remarks

This phylogeographic study of the mycoheterotrophic *A. uniflora* revealed a clear genetic divergence between Bolivian-Peruvian and Andean-Patagonian populations since the Late Miocene, in correlation with the formation of the Arid Diagonal caused by the Andes uplift. Long distance dispersal was not supported. The current distribution range in Patagonia had been already achieved, at least through two colonization pulses, before the GPG, i.e. in the early Pleistocene. Thus, we inferred that ancient geological events and the consequently associated climatic changes were the main drivers of current genetic diversity patterns as was seen in other organisms (Hoorn et al., 2010; Acosta et al., 2014). Early Pleistocene glaciations were mostly responsible for the last haplotype diversifications and the arrival of the species in the Malvinas Islands through putative land bridges. Instead, LGM had a smaller

influence on the retrieved patterns. High genetic diversity areas revealed *in situ* persistence during glaciations, suggesting that *A. uniflora* is a cold-tolerant species; those areas are remarkably coincident with those recovered for its fungal symbiont (Renny et al., 2017).

Supplementary data to this article can be found online at https://doi.org/10.1016/j.gloplacha.2021.103701.

Funding information

This work was supported by the National Research Council of Argentina [grant numbers PIP 201101-00245, PIP 11220150100690CO; to A.N.S.]; and by the National Ministry of Science and Technology [grant numbers FONCYT-PICT-2011-0837, PICT 2015-3089; to A.N.S.]. Authors declare no conflicts of interest to report.

Declaration of Competing Interest

Authors Mauricio Renny, M. Cristina Acosta, and Alicia N. Sérsic declare no conflicts of interest to report.

Acknowledgments

We thank L. Domínguez, M. Strelin, A. A. Cocucci, A. Cosacov, M. Baranzelli, G. Ferreiro and F. Sazatornil for field assistance, and L. Caeiro for Lab assistance; we also thank the National Parks Administration (APN, Argentina; n° 014/2012, and n° 1172/2013) and National Forest Corporation (CONAF, Chile; n° 93/2013) for sampling permissions. We especially thank V. Merckx for outgroup samples, and C. Martel and M. Bidartondo for providing *A. uniflora* specimens from Peru and Malvinas Islands, respectively. We thank anonymous reviewers and Editor for their comments and suggestions, which improved the manuscript. M.C.A. and A.N.S. are researchers in National Research Council of Argentina (CONICET).

References

Acosta, M.C., Mathiasen, P., Premoli, A.C., 2014. Retracing the evolutionary history of *Nothofagus* in its geo-climatic context: new developments in the emerging field of phylogeology. Geobiology 12, 497–510.
Allouche, O., Tsoar, A., Kadmon, R., 2006. Assessing the accuracy of species distribution models: prevalence, kappa and the true skill statistic (TSS). J. Appl. Ecol. 43, 1223–1232.
Ammann, C., Jenny, B., Kammer, K., Messerli, B., 2001. Late Quaternary Glacier response to humidity changes in the arid Andes of Chile (18–29° S). Palaeogeogr. Palaeoclimatol. Palaeoecol. 172, 313–326.
Anderson, R.P., Gómez-Laverde, M., Peterson, A.T., 2002. Geographical distributions of spiny pocket mice in South America: insights from predictive models. Glob. Ecol. Biogeogr. 11, 131–141.
Bacon, C.D., Velásquez-Puentes, F.J., Hinojosa, L.F., Schwartz, T., Oxelman, B., Pfeil, B., Arroyo, M.T.K., Wanntorp, L., Antonelli, A., 2018. Evolutionary persistence in Gunnera and the contribution of southern plant groups to the tropical Andes biodiversity hotspot. PeerJ 6, e4388.
Bandelt, H.J., Forster, P., Röhl, A., 1999. Median-joining networks for inferring intraspecific phylogenies. Mol. Biol. Evol. 16, 37–48.
Baranzelli, M.C., Johnson, L.A., Cosacov, A., Sérsic, A.N., 2014. Historical and ecological divergence among populations of *Monttea chilensis* (Plantaginaceae), an endemic endangered shrub bordering the Atacama Desert, Chile. Evol. Ecol. 28, 751–774.
Baranzelli, M.C., Cosacov, A., Ferreiro, G., Johnson, L.A., Sérsic, A.N., 2017. Travelling to the south: Phylogeographic spatial diffusion model in *Monttea aphylla* (Plantaginaceae), an endemic plant of the Monte Desert. PLoS One 12, e0178827.
Baranzelli, M.C., Cosacov, A., Espíndola, A., et al., 2018. Echoes of the whispering land: interacting roles of vicariance and selection in shaping the evolutionary divergence of two Calceolaria (Calceolariaceae) species from Patagonia and Malvinas/Falkland Islands. Evol. Ecol. 32, 287–314.
Barreda, V.D., 1996. Bioestratigrafía de polen y esporas de la Formacion Chenque, Oligoceno tardío? Mioceno de las Provincias de Chubut y Santa Cruz, Patagonia, Argentina. Ameghiniana 33, 35–56.
Barrett, C.F., Freudenstein, J.V., 2011. An integrative approach to delimiting species in a rare but widespread mycoheterotrophic orchid. Mol. Ecol. 20, 2771–2786.
Barve, N., Barve, V., Jiménez-Valverde, A., et al., 2011. The crucial role of the accessible area in ecological niche modeling and species distribution modeling. Ecol. Model. 222, 1810–1819.
Bechis, F., Encinas, A., Concheyro, A., Litvak, V.D., Aguirre-Urreta, B., Ramos, V.A., 2014. New age constraints for the Cenozoic marine transgressions of northwestern Patagonia, Argentina (41° - 43° S): Paleogeographic and tectonic implications. J. S. Am. Earth Sci. 52, 72–93.
Bell, C.D., Kutschker, A., Arroyo, M.T.K., 2012. Phylogeny and diversification of Valerianaceae (Dipsacales) in the southern Andes. Mol. Phylogenet. Evol. 63, 724–737.
Bidartondo, M.I., Redecker, D., Hijri, I., et al., 2002. Epiparasitic plants specialized on arbuscular mycorrhizal fungi. Nature 419, 389–392.
Bielejec, F., Rambaut, A., Suchard, M.A., Lemey, P., 2011. SPREAD: spatial phylogenetic reconstruction of evolutionary dynamics. Bioinformatics 27, 2910–2912.
Brown, J.L., Hill, D.J., Dolan, A.M., Carnaval, A.C., Haywood, A.M., 2018. PaleoClim, high spatial resolution paleoclimate surfaces for global land areas. Scientific Data 5, 1–9.
Busby, J.R., 1991. BIOCLIM A bioclimate analysis and prediction system. In: Margules, C. R., Austin, M.P. (Eds.), Nature Conservation: Cost Effective Biological Surveys and Data Analysis. CSIRO, Canberra, pp. 64–68.
Camps, G.A., Martínez-Meyer, E., Verga, A.R., Sérsic, A.N., Cosacov, A., 2018. Genetic and climatic approaches reveal effects of Pleistocene refugia and climatic stability in an old giant of the Neotropical Dry Forest. Biol. J. Linn. Soc. 20, 1–20.
Carpenter, G., Gillison, A.N., Winter, J., 1993. DOMAIN: a flexible modelling procedure for mapping potential distributions of plants and animals. Biodivers. Conserv. 2, 667–680.
Chase, M.W., Soltis, D.E., Olmstead, R.G., et al., 1993. Phylogenetics of seed plants: an analysis of nucleotide sequences from the plastid gene rbcL. Ann. Mo. Bot. Gard. 528–580.
Clayton, J.D., Clapperton, C.M., 1997. Broad Synchrony of a Late-Glacial Glacier Advance and the Highstand of Palaeolake Tauca in the Bolivian Altiplano. J. Quat. Sci. 12, 169–182.
Cohen, J., 1960. A coefficient of agreement of nominal scales. Educ. Psychol. Meas. 20, 37–46.
Coronato, A.M.J., Martínez, O., Rabassa, J., 2004. Glaciations in argentine Patagonia, southern South America. In: Developments in Quaternary Sciences, vol. 2. Elsevier, Oxford, pp. 49–67.
Coronato, A.M.J., Coronato, F., Mazzoni, E., Vázquez, M., 2008. The Physical Geography of Patagonia and Tierra del Fuego. Developments in Quaternary Sciences 11, 13–55.
Cosacov, A., Sérsic, A.N., Sosa, V., De-Nova, A., Nylinder, S., Cocucci, A., 2009. New insights in the phylogenetic relationships, character evolution, and biogeography of Calceolaria (Calceolariaceae). Am. J. Bot. 96, 2240–2255.
Crandall, K.A., Templeton, A.R., 1993. Empirical tests of some predictions from coalescent theory with applications to intraspecific phylogeny reconstruction. Genetics 134, 959–969.
Darriba, D., Taboada, G.L., Doallo, R., Posada, D., 2012. jModelTest 2: more models, new heuristics and parallel computing. Nat. Methods 9, 772.
Davis, M.B., Shaw, R.G., 2001. Range shifts and adaptive responses to Quaternary climate change. Science 292, 673–679.
DePamphilis, C.W., Young, N.D., Wolfe, A.D., 1997. Evolution of plastid gene rps2 in a lineage of hemiparasitic and holoparasitic plants: many losses of photosynthesis and complex patterns of rate variation. Proc. Natl. Acad. Sci. 94, 7367–7372.
Dimitri, M.J., 1972. Una nueva especie del género Arachnitis Phil. (Corsiaceae). Revista Facultad de Agronomía de la Universidad Nacional de La Plata 48, 37–45.
Do, H.D.K., Kim, C., Chase, M.W., Kim, J.H., 2020. Implications of plastome evolution in the true lilies (monocot order Liliales). Mol. Phylogenet. Evol. 148, 106818.
Domínguez, L.S., Sérsic, A., 2004. The southernmost myco-heterotrophic plant, Arachnitis uniflora: root morphology and anatomy. Mycologia 96, 1143–1151.
Drummond, A.J., Rambaut, A., 2007. BEAST: Bayesian evolutionary analysis by sampling trees. BMC Evol. Biol. 7, 214.
Drummond, A.J., Rambaut, A., Shapiro, B., Pybus, O.G., 2005. Bayesian coalescent inference of past population dynamics from molecular sequences. Mol. Biol. Evol. 22, 1185–1192.
Dupanloup, I., Schneider, S., Excoffier, L., 2002. A simulated annealing approach to define the genetic structure of populations. Mol. Ecol. 11, 2571–2581.
Excoffier, L., 2004. Patterns of DNA sequence diversity and genetic structure after a range expansion: lessons from the infinite-island model. Mol. Ecol. 13, 853–864.
Excoffier, L., Laval, G., Schneider, S., 2005. Arlequin version 3.01: an integrated software package for population genetics data analysis. Evol. Bioinformatics Online 1, 47–60.
Ezcurra, C., 2002. Phylogeny, Morphology, and Biogeography of Chuquiraga, an Andean-Patagonian Genus of Asteraceae-Barnadesioideae. Bot. Rev. 68, 153–170.
Farber, O., Kadmon, R., 2003. Assessment of alternative approaches for bioclimatic modeling with special emphasis on the Mahalanobis distance. Ecol. Model. 160, 115–130.
Fielding, A.H., Bell, J.F., 1997. A review of methods for the assessment of prediction errors in conservation presence/absence models. Environ. Conserv. 24, 38–49.
Fu, Y.X., 1997. Statistical tests of neutrality of mutations against population growth, hitchhiking and background selection. Genetics 147, 915–925.
Graf, K., 1992. Pollendiagramme aus den Anden, eine Synthese zur Klimageschichte und Vegetationsentwicklung seit der letzten Eiszeit. Phys. Geogr. 34, 1–138.
Graham, A., 2009. The Andes: a geological overview from a biological perspective. Ann. Mo. Bot. Gard. 96, 371–385.
Guisan, A., Edwards Jr., T.C., Hastie, T., 2002. Generalized linear and generalized additive models in studies of species distributions: setting the scene. Ecol. Model. 157, 89–100.
Heibl, C., Renner, S.S., 2012. Distribution models and a dated phylogeny for Chilean Oxalis species reveal occupation of new habitats by different lineages, not rapid adaptive radiation. Syst. Biol. 61, 823–834.
Hewitt, G.M., 1996. Some genetic consequences of ice ages, and their role in divergence and speciation. Biol. J. Linn. Soc. 58, 247–276.

Hoorn, C., Wesselingh, F.P., ter Steege, H., et al., 2010. Amazonia through time: Andean uplift, climate change, landscape evolution, and biodiversity. Science 330, 927–931.
Hueck, K., 1978. Los bosques de Sudamérica. GTZ, Eschborn, Alemania.
Hutchinson, D.W., Templeton, A.R., 1999. Correlation of Pairwise Genetic and Geographic Distance measures: Inferring the Relative Influences of Gene Flow and Drift on the distribution of Genetic Variability. Evolution 53, 1898–1914.
Ibisch, P.L., Neinhuis, C., Rojas, P.N., 1996. On the biology, biogeography, and taxonomy of Arachnitis Phil. Nom. Cons. (Corsiaceae) in respect to a new record from Bolivia. Willdenowia 26, 321–332.
Karatzoglou, A., Smola, A., Hornik, K., Zeileis, A., 2004. kernlab - An S4 Package for Kernel Methods in R. J. Stat. Softw. 11, 1–20.
Kull, C., Grosjean, M., 2000. Late Pleistocene climate conditions in the North Chilean Andes drawn from a climate– glacier model. J. Glaciol. 46, 622–632.
Kuzoff, R.K., Sweere, J.A., Soltis, D.E., Soltis, P.S., Zimmer, E.A., 1998. The phylogenetic potential of entire 26S rDNA sequences in plants. Mol. Biol. Evol. 15, 251–263.
Lavenu, A., 1986. Etude neotectonique de l' Altiplano et de la Cordillere Orientale des Andes boliviennes. PhD Thesis. Université de Paris, Sud. France.
Lemaire, B., Huysmans, S., Smets, E., Merckx, V., 2011. Rate accelerations in nuclear 18S rDNA of mycoheterotrophic and parasitic angiosperms. J. Plant Res. 124, 561–576.
Lemey, P., Rambaut, A., Welch, J.J., Suchard, M.A., 2010. Phylogeography takes a relaxed random walk in continuous space and time. Mol. Biol. Evol. 27, 1877–1885.
Liaw, A., Wiener, M., 2002. Classification and regression by randomForest. R News 2, 18–22.
Linder, H., 2008. Plant species radiations: where, when, why? Philosophical Transactions of the Royal Society B: Biological Sciences 1506, 3097–3105.
Luebert, F., Weigend, M., 2014. Phylogenetic insights into Andean plant diversification. Front. Ecol. Evol. 2 https://doi.org/10.3389/fevo.2014.00027.
Luebert, F., Hilger, H.H., Weigend, M., 2011. Diversification in the Andes: Age and origins of South American Heliotropium lineages (Heliotropiaceae, Boraginales). Mol. Phylogenet. Evol. 61, 90–102.
Mark, B.G., Harrison, S.P., Spessa, A., New, M., Evans, D.J.A., Helmens, K.F., 2005. Tropical snowline changes at the last Glacial Maximum: a global assessment. Quat. Int. 138, 168–201.
McCormack, J.E., Hird, S.M., Zellmer, A.J., Carstens, B.C., Brumfield, R.T., 2013. Applications of next-generation sequencing to phylogeography and phylogenetics. Mol. Phylogenet. Evol. 66, 526–538.
Mennes, C.B., Lam, V.K.Y., Rudall, P.J., et al., 2015. Ancient Gondwana break-up explains the distribution of the mycoheterotrophic family Corsiaceae (Liliales). J. Biogeogr. 42, 1123–1136.
Merckx, V., Freudenstein, J.V., Kissling, J., et al., 2013a. Taxonomy and classification. In: Merckx, V. (Ed.), Mycoheterotrophy. The Biology of Plants Living on Fungi. Springer, London, pp. 19–101.
Merckx, V., Mennes, C.B., Peay, K.G., Geml, J., 2013b. Evolution and diversification. In: Merckx, V. (Ed.), Mycoheterotrophy. The Biology of Plants Living on Fungi. Springer, London, pp. 215–244.
Merckx, V.S.F.T., Gomes, S.I.F., Wapstra, M., et al., 2017. The biogeographical history of the interaction between mycoheterotrophic Thismia (Thismiaceae) plants and mycorrhizal Rhizophagus (Glomeraceae) fungi. J. Biogeogr. 44, 1869–1879.
Miller, M.P., 2005. Alleles in space: computer software for the joint analysis of interindividual spatial and genetic information. J. Hered. 96, 722–724.
Mörner, N.A., Sylwan, C., 1989. Magnetostratigraphy of the Patagonian moraine sequence at Lago Buenos Aires. J. S. Am. Earth Sci. 2, 385–389.
Muscarella, R., Galante, P.J., Soley-Guardia, M., et al., 2017. Package "ENMeval," version 0.3.0.
Nei, M., 1987. Molecular Evolutionary Genetics. Columbia University Press, New York.
Nickrent, D.L., Ouyang, Y., Duff, R.J., Depamphilis, C.W., 1997. Do nonasterid holoparasitic flowering plants have plastid genomes? Plant Mol. Biol. 34, 717–729.
Nylander, J.A.A., 2004. MrModeltest V.2. Program Distributed by the Author. Uppsala University, Sweden.
Ochoa, J.G., Collantes, B., Martel, C., 2019. Arachnitis uniflora: first report of Corsiaceae for the Peruvian Flora. Kew Bull. 74, 43.
O'Driscoll, L.J., Richards, M.A., Humphreys, E.D., 2012. Nazca–South America interactions and the late Eocene–late Oligocene flat-slab episode in the central Andes. Tectonics 31, 1–16.
Ortiz-Jaureguizar, E., Cladera, G.A., 2006. Palaeoenvironmental evolution of southern South America during the Cenozoic. J. Arid Environ. 66, 498–532.
Osorio-Olvera, L., Barve, V., Barve, N., Soberón, J., 2016. nichetoolbox: From getting biodiversity data to evaluating species distribution models in a friendly GUI environment. R package version 0.1.6.0. Available at: http://shiny.conabio.gob.mx:3838/nichetoolb2/.
Palazzesi, L., Barreda, V., 2012. Fossil pollen records reveal a late rise of open-habitat ecosystems in Patagonia. Nat. Commun. 3, 1294.
Panti, C., 2011. Palaeofloristic analysis of the Río Guillermo Formation (late Eocene–early Oligocene?), Santa Cruz, Argentina. Ameghiniana 48, 320–335.
Peterson, A.T., Papes, M., Soberon, J., 2008. Rethinking receiver operating characteristic analysis applications in ecological niche modeling. Ecol. Model. 213, 63–72.
Phillips, S.J., Anderson, R.P., Schapire, R.E., 2006. Maximum entropy modeling of species geographic distributions. Ecol. Model. 190, 231–259.
Premoli, A.C., Mathiasen, P., Kitzberger, T., 2010. Southern-most Nothofagus trees enduring ice ages: genetic evidence and ecological niche retrodiction reveal high latitude (54°S) glacial refugia. Palaeogeogr. Palaeoclimatol. Palaeoecol. 298, 247–256.
Premoli, A.C., Mathiasen, P., Acosta, M.C., Ramos, V.A., 2012. Phylogeographically concordant intraspecific cpDNA divergence in sympatric *Nothofagus*. How deep can it be? New Phytol. 193, 261–275.
Quiroga, M.P., Mathiasen, P., Iglesias, A., Mill, R.R., Premoli, A.C., 2015. Molecular and fossil evidence disentangle the biogeographical history of *Podocarpus*, a key genus in plant geography. J. Biogeogr. 43, 372–383.
Rabassa, J., 2008. Late Cenozoic Glaciations in Patagonia and Tierra del Fuego. Developments in Quaternary Sciences 11, 151–204.
Rabassa, J., Coronato, A., Martínez, O., 2011. Late Cenozoic glaciations in Patagonia and Tierra del Fuego: an updated review. Biol. J. Linn. Soc. 103, 316–335.
Ramos, V.A., Ghiglione, M.C., 2008. Tectonic evolution of the Patagonian Andes. In: Rabassa, J. (Ed.), The Late Cenozoic of Patagonia and Tierra del Fuego, Developments in Quaternary Sciences, vol. 11. Elsevier, Oxford, pp. 57–71.
Renny, M., Acosta, M.C., Cofré, N., Domínguez, L.S., Bidartondo, M.I., Sérsic, A.N., 2017. Genetic diversity patterns of arbuscular mycorrhizal fungi associated with the mycoheterotroph *Arachnitis uniflora* Phil (Corsiaceae). Ann. Bot. 119, 1279–1294.
Rodríguez, F., Oliver, J.L., Marín, A., Medina, J.R., 1990. The general stochastic model of nucleotide substitution. J. Theor. Biol. 142, 485–501.
Rogers, A.R., Harpending, H., 1992. Population growth makes waves in the distribution of pairwise genetic differences. Mol. Biol. Evol. 9, 552–569.
Romero, E.J., 1986. Paleogene phytogeography and climatology of South America. Ann. Mo. Bot. Gard. 73, 449–461.
Ronquist, F., Huelsenbeck, J., 2003. MrBayes 3: Bayesian phylogenetic inference under mixed models. Bioinformatics 19, 1572–1574.
Rozas, J., Sanchez-DelBarrio, J.C., Messeguer, X., Rozas, R., 2003. DnaSP, DNA polymorphism analyses by the coalescent and other methods. Bioinformatics 19, 2496–2497.
Seltzer, G.O., 1992. Late Quaternary glaciation of the Cordillera real, Bolivia. J. Quat. Sci. 7, 87–98.
Sérsic, A.N., Cosacov, A., Cocucci, A.A., et al., 2011. Emerging phylogeographical patterns of plants and terrestrial vertebrates from Patagonia. Biol. J. Linn. Soc. 103, 475–494.
Slater, G.J., Thalmann, O., Leonard, J.A., et al., 2009. Evolutionary history of the Falklands wolf. Current Biology Magazine 19, R937–R938.
Soberón, J., 2007. Grinnellian and Eltonian niches and geographic distributions of species. Ecol. Lett. 10, 1115–1123.
Soberón, J., Peterson, A.T., 2005. Interpretation of models of fundamental ecological niches and species' distributional areas. Biodivers. Inform. 2, 1–10.
Souto, C.P., Premoli, A.C., 2007. Genetic variation in the widespread *Embothrium coccineum* (Proteaceae) endemic to Patagonia: effects of phylogeny and historical events. Aust. J. Bot. 55, 809–817.
Souto, C.P., Mathiasen, P., Acosta, M.C., et al., 2015. Identifying genetic hotspots by mapping molecular diversity of widespread trees: when commonness matters. J. Hered. 106, 537–545.
Sun, Y., Skinner, D.Z., Liang, G.H., Hulbert, S.H., 1994. Phylogenetic analysis of Sorghum and related taxa using internal transcribed spacers of nuclear ribosomal DNA. Theor. Appl. Genet. 89, 26–32.
Tajima, F., 1989. The effect of change in population size on DNA polymorphism. Genetics 123, 598–601.
Tamura, K., Stecher, G., Peterson, D., Filipski, A., Kumar, S., 2013. MEGA6: molecular evolutionary genetics analysis version 6.0. Mol. Biol. Evol. 30, 2725–2729.
Ton-That, T., Singer, B., Mörner, N.A., Rabassa, J., 1999. Datación por el método 40Ar/39Ar de lavas basálticas y geología del Cenozoico Superior en la región del Lago Buenos Aires, provincia de Santa Cruz, Argentina. Asociación Geológica Argentina 54, 333–352.
Vergara, R., Gitzendanner, M.A., Soltis, D.E., Soltis, P.S., 2014. Population genetic structure, genetic diversity, and natural history of the South American species of *Nothofagus* subgenus *Lophozonia* (Nothofagaceae) inferred from nuclear microsatellite data. Ecology and Evolution 4, 2450–2471.
Villagrán, C., Hinojosa, L.F., 1997. Historia de los bosques del sur de Sudamérica, II: Análisis fitogeográfico. Rev. Chil. Hist. Nat. 70, 241–267.
White, T.J., Bruns, T., Lee, S.B., Taylor, J.W., 1990. Amplification and direct sequencing of fungal ribosomal RNA genes for phylogenetics. In: Innis, M.A., Gelfand, D.H., Sninsky, J.J., White, T.J. (Eds.), PCR Protocols. Academic Press, New York, pp. 315–322.
Wilf, P., Cúneo, N.R., Escapa, I.H., Pol, D., Woodburne, M.O., 2013. Splendid and seldom Isolated: the Paleobiogeography of Patagonia. Annu. Rev. Earth Planet. Sci. 41, 561–603.
Wilkie, S., 1997. Isolation of total genomic DNA. In: Clark, M.S. (Ed.), Plant Molecular Biology - a Laboratory Manual. Springer-Verlag, Berlín, pp. 3–15.
Yrigoyen, M.R., 1979. Cordillera principal. In: Actas del II Simposio de Geología Regional. Córdoba, Argentina, pp. 651–694.
Zachos, J.C., Dickens, G.R., Zeebe, R.E., 2008. An early Cenozoic perspective on greenhouse warming and carbon-cycle dynamics. Nature 451, 279–283.